

JAERI - M
86-033

CONFINEMENT STUDIES DURING THE ICRF HEATING
EXPERIMENT IN THE JFT-2M

March 1986

Kazuo ODAJIMA, Hiroshi MATSUMOTO, Hiroshi TAMAI,
Toshihide OGAWA, Katsumichi HOSHINO, Satoshi KASAI,
Tomohide KAWAKAMI, Hisato KAWASHIMA, Tohru MATOBA,
Toshiaki MATSUDA, Yukitoshi MIURA, Masahiro MORI,
Hiroaki OGAWA, Hideo OHTSUKA, Seio SENGOKU, Teruaki SHOJI,
Norio SUZUKI, Yoshihiko UESUGI, Takumi YAMAMOTO,
Toshihiko YAMAUCHI, Mitsuru HASEGAWA*, Susumu TAKADA**
and Ichiro YANAGISAWA***

日本原子力研究所
Japan Atomic Energy Research Institute

JAERI-Mレポートは、日本原子力研究所が不定期に公刊している研究報告書です。
入手の問い合わせは、日本原子力研究所技術情報部情報資料課（〒319-11茨城県那珂郡東海村）あて、お申しこしください。なお、このほかに財団法人原子力弘済会資料センター（〒319-11茨城県那珂郡東海村日本原子力研究所内）で複写による実費頒布をおこなっております。

JAERI-M reports are issued irregularly.

Inquiries about availability of the reports should be addressed to Information Division
Department of Technical Information, Japan Atomic Energy Research Institute, Tokai-
mura, Naka-gun, Ibaraki-ken 319-11, Japan.

©Japan Atomic Energy Research Institute, 1986

編集兼発行 日本原子力研究所
印刷 髙野高速印刷

Confinement Studies During the ICRF Heating Experiment in the JFT-2M.

Kazuo ODAJIMA, Hiroshi MATSUMOTO, Hiroshi TAMAI, Toshihide OGAWA,
Katsumichi HOSHINO, Satoshi KASAI, Tomohide KAWAKAMI, Hisato KAWASHIMA,
Tohru MATOBA, Toshiaki MATSUDA, Yukitoshi MIURA, Masahiro MORI,
Hiroaki OGAWA, Hideo OHTSUKA, Seio SENGOKU, Teruaki SHOJI, Norio SUZUKI,
Yoshihiko UESUGI, Takumi YAMAMOTO, Toshihiko YAMAUCHI, Mitsuru HASEGAWA*,
Susumu TAKADA** and Ichiro YANAGISAWA***

Department of Thermonuclear Fusion Research,
Naka Fusion Research Establishment
Japan Atomic Energy Research Institute,
Naka-Machi, Naka-Gun, Ibaraki-Ken

(Received January 31, 1986)

Decay time of stored energy when additional heating power decreased abruptly is measured. The energy decay time is almost constant 15 ms irrespective of the gross energy confinement time $\tau_E^G = 21 - 46$ ms, which are changed by the ICRF heating power up to 1.5 MW. The decay time coincides with a confinement time of the additionally heated power defined by $\tau_{ad} = \Delta W_T / P_{Tot} | \frac{1}{n_e} = \text{const}$. This results indicates that the incremental energy by the additional heating behaves independently of the gross plasma energy. It is also shown that τ_{ad} is almost independent of density and plasma current as well as heating power.

Keywords: JFT-2M Tokamak, ICRF Heating, NBI Heating, Confinement Scaling,
Tokamak, Additional Heating, Energy Confinement Time

* On leave from Mitsubishi Electric Co.

** On leave from Mitsubishi Computer System Tokyo Co.

*** On leave from Mitsubishi Atomic Power Industries Inc.

JFT-2MにおけるICRF加熱時のプラズマの
エネルギー閉じ込め特性

日本原子力研究所那珂研究所核融合研究部

小田島和男・松本 宏・玉井広史・小川俊英・星野克道
河西 敏・河上知秀・川島寿人・的場 徹・松田俊明
三浦幸俊・森 雅博・小川宏明・大塚英男・仙石盛夫
荘司昭朗・鈴木紀男・上杉喜彦・山本 巧・山内俊彦
長谷川満*・高田 晋**・柳沢一郎***

(1986年1月31日受理)

追加熱を遮断したときのプラズマの蓄積エネルギーの減衰時間を測定し、プラズマの全エネルギーを全加熱入力で割った全閉じ込め時間と比較した。その結果全閉じ込め時間を20~40 msと大幅に変えても、エネルギーの減衰時間は15msと変らなかった。この減衰時間は、追加熱によって増えた分のエネルギー閉じ込め時間 $\tau_{ad} = 4W_T / 4P_{Tot} | \bar{n}_e = \text{const.}$ と一致する。この結果は追加熱によって増えた分のプラズマは、全体のプラズマと独立して損失していることを示している。従って、将来の高加熱入力時における蓄積エネルギー、又は全閉じ込め時間を予測するためには、この τ_{ad} の比例則を確立することが重要である。本論文で確かめられた比例則は、

$$\tau_{ad} \propto I_p^0 \cdot \bar{n}_e^0 \cdot P_{ad}^0$$

である。

那珂研究所：茨城県那珂郡那珂町大字向山

* 外来研究員，三菱電機（株）

** # 三菱電機東部コンピューターシステム（株）

*** 三菱原子力（株）

Contents

1. Introduction	1
2. Experimental Condition	2
3. Experimental Results	3
3.1 General feature of heating	3
3.2 Dependence on Density and Plasma current	4
3.3 Transient Characteristic of the Stored Energy	5
3.4 Confinement Model and Point Model Simulation	6
3.5 Improved Confinement Case	7
4. Discussion and Summary.	8
4.1 Cause of Confinement Deterioration	8
4.2 Effect of Plasma Current	9
4.3 Validity of two Plasma Model	9
4.4 Summary	9
Acknowledgement	10
References	11

目 次

1. 序文	1
2. 実験条件	2
3. 実験結果	3
3.1 加熱プラズマ	3
3.2 プラズマの密度と電流に対する依存性	4
3.3 蓄積エネルギーの過渡特性	5
3.4 閉じ込めのモデルとシミュレーション	6
3.5 閉じ込めの改善	7
4. 議論とまとめ	8
4.1 閉じ込めの劣化の原因	8
4.2 プラズマ電流の効果	9
4.3 2つのプラズマモデルの有効性	9
4.4 まとめ	9
謝辞	10
参考文献	11

1. INTRODUCTION

ICRF heating has experimentally been successfully demonstrated in many medium size and big tokamaks [1-5]. A main interest in the ICRF heating experiment is moved to a confinement study in a high power heating regime. Systematic scaling experiment showed a deterioration of a gross energy confinement with strong NBI heating, where the gross energy confinement time is defined by $\tau_E^G = W_T/P_{Tot}$, where W_T is total stored energy and P_{Tot} is total input power. In the case of ICRF heating, almost the same deterioration as NBI heating of confinement time are observed [1-5]. An attempt to scale the gross energy confinement time is summarized, for example, Kaye-Goldston scaling, as following [6].

$$\tau_E^G = 2.77 \times 10^{-5} k^{0.28} B_T^{-0.09} I_p^{1.24} P_{Tot}^{-0.58} n_e^{0.26} a^{-0.49} R^{1.65}$$

The definition and the unit of each notation is described in the next section.

On the other hand, many heating experiments in tokamaks show that the total stored kinetic energy increases linearly as the additional heating power although the line does not go through the origin indicating degradation of gross energy confinement time compared to the ohmic phase. One is tempted then to conclude that some sort of "incremental" confinement time τ_{ad} does not deteriorate with increasing input power [7], but physical meaning of the τ_{ad} is not clear on the point of view of energy transport study.

Recently, some experiments which change our understandings on a transport inside a plasma are presented. That is so called "Profile consistency", where the gross energy confinement time and electron temperature profile are independent on the heating power deposition. The plasma maintains the optimum current density profile by changing its transport properties [7-9]. This suggests us the possibility that the displacement from the ohmic equilibrium behaves independently of the ohmic base plasma.

In this paper, confinement studies during the ICRF heating are presented with an attention to the change of total stored energy. An important result pointed out in this paper is that a characteristic time of the total stored energy decrease (or increase) is almost constant 15ms and is independent of the gross energy confinement time. Therefore, the definition of energy confinement time τ_E^G ,

$$\frac{dW_T}{dt} = P_{Tot} - \frac{W_T}{\tau_E} \quad (1)$$

is not suitable in the additionally heated plasma. The plasma can be considered to consist of two parts, those are, ohmic base plasma and increment part by the ICRF heating. The cause of the apparent deterioration in the gross energy confinement time is that the incremental energy confinement time is small compared to that of ohmic base plasma.

In the following section, experimental conditions are presented. In section 3, experimental results, which include measurements of energy decay times in a plasma where the gross energy confinement time changes from 46ms to 20ms. The final section, the results are discussed and summarized.

2. EXPERIMENTAL CONDITIONS

The JFT-2M is a tokamak with D shaped vacuum vessel with 1.31 m major radius and 0.415×0.595 m minor radii. In the present experiment, the machine is operated with D shaped cross section and the plasma radius is limited by inner and outer limiters at $a_L = 0.35$ m. The main parameters are summarized as follows;

minor radius	$a = 0.34$ m
major radius	$R = 1.3$ m
ellipticity	$\kappa = 1.4 \sim 1.5$
triangularity	$\delta = 0.15 \sim 0.25$
plasma current	$I_p = 0.2 \sim 0.45$ MA
magnetic field	$B_T = 1.15 \sim 1.2$ T

The rf generator is operated at a frequency 15.4 MHz which is fundamental cyclotron frequency of protons at $B_T = 1.0$ T. An array of three loop antennae on the high field side is used. The length of the radiative part is 0.5 m and the width of the central conductor is 7 cm. The distance between the top of limiter and the center conductor is 2 cm. A double or single layer Faraday shield is made of titanium, and the side protection of the Faraday shield is carbon. The limiter is also made of carbon graphite.

The antenna array is operated at out of phase, that is, antenna current at center element is out of phase respect to both side elements. Using the out of phase operation, impurity contamination due to the rf

$$\frac{dW_T}{dt} = P_{Tot} - \frac{W_T}{\tau_E G} \quad (1)$$

is not suitable in the additionally heated plasma. The plasma can be considered to consist of two parts, those are, ohmic base plasma and increment part by the ICRF heating. The cause of the apparent deterioration in the gross energy confinement time is that the incremental energy confinement time is small compared to that of ohmic base plasma.

In the following section, experimental conditions are presented. In section 3, experimental results, which include measurements of energy decay times in a plasma where the gross energy confinement time changes from 46ms to 20ms. The final section, the results are discussed and summarized.

2. EXPERIMENTAL CONDITIONS

The JFT-2M is a tokamak with D shaped vacuum vessel with 1.31 m major radius and 0.415×0.595 m minor radii. In the present experiment, the machine is operated with D shaped cross section and the plasma radius is limited by inner and outer limiters at $a_L = 0.35$ m. The main parameters are summarized as follows;

minor radius	$a = 0.34$ m
major radius	$R = 1.3$ m
ellipticity	$\kappa = 1.4 \sim 1.5$
triangularity	$\delta = 0.15 \sim 0.25$
plasma current	$I_p = 0.2 \sim 0.45$ MA
magnetic field	$B_T = 1.15 \sim 1.2$ T

The rf generator is operated at a frequency 15.4 MHz which is fundamental cyclotron frequency of protons at $B_T = 1.0$ T. An array of three loop antennae on the high field side is used. The length of the radiative part is 0.5 m and the width of the central conductor is 7 cm. The distance between the top of limiter and the center conductor is 2 cm. A double or single layer Faraday shield is made of titanium, and the side protection of the Faraday shield is carbon. The limiter is also made of carbon graphite.

The antenna array is operated at out of phase, that is, antenna current at center element is out of phase respect to both side elements. Using the out of phase operation, impurity contamination due to the rf

heating is sufficiently suppressed to obtain a high density plasma[1,10].

RF power coupled to the plasma P_{ICH} is defined by

$$P_{\text{ICH}} = \frac{R_P - R_V}{R_P} P_G = \eta P_G \quad (2)$$

where P_G is generator output power and η is coupling efficiency. R_V and R_P are antenna loading resistance for without and with plasma defined by $R = P_G/I_A^2$, respectively, where I_A is rf current at the antenna. These three antenna elements have R_V values in the range of 0.3Ω at 15.4 MHz, and R_P increases as plasma density. The coupling efficiency changes from 50 % at low density to 75 % at high density region.

A total stored energy is determined by a magnetic field fitting method[11] using 24 magnetic probes and 8 saddle loops, where a value of $\Lambda = \beta_p + (l_i - 1)/2$ is obtained, where β_p is poloidal beta value and l_i is internal inductance of the plasma. The value of l_i is determined as follows; assuming that the stored energy in ohmic plasma is proportional to a line average electron density \bar{n}_e , Λ is plotted as a function of \bar{n}_e and the Λ value at the extrapolated straight line with $\bar{n}_e = 0$ is assumed $\beta_p = 0$.

3. EXPERIMENTAL RESULTS.

3.1 General feature of heating

Temporal evolution of the plasma parameters during 1.2 MW ICRF heating is shown in Fig. 1. The plasma current is 225 kA and $\kappa = 1.2$. The density increases from 3 to $5 \times 10^{19} \text{ m}^{-3}$ during the heating pulse due to intense gas puffing. The loop voltage decreases from 1.7 to 0.8 V. The central electron temperature measured by Thomson scattering increases from 0.8 keV just before the heating to 1.9 keV at peak value and then decreases gradually. The poloidal beta value, however, continues increasing during the heating pulse. Therefore, the decay of the electron temperature is considered to be the results of the rapid increase of electron density. The deuterium temperature measured by a mass separated charge exchange neutral analyser increases from 0.5 to 0.9 keV, the increment is much smaller compared to the increase of electron temperature. This results indicates that strong electron heating occurs as is expected from mode conversion theory[12].

heating is sufficiently suppressed to obtain a high density plasma[1,10].

RF power coupled to the plasma P_{ICH} is defined by

$$P_{\text{ICH}} = \frac{R_P - R_V}{R_P} P_G = \eta P_G \quad (2)$$

where P_G is generator output power and η is coupling efficiency. R_V and R_P are antenna loading resistance for without and with plasma defined by $R = P_G/I_A^2$, respectively, where I_A is rf current at the antenna. These three antenna elements have R_V values in the range of 0.3Ω at 15.4 MHz, and R_P increases as plasma density. The coupling efficiency changes from 50 % at low density to 75 % at high density region.

A total stored energy is determined by a magnetic field fitting method[11] using 24 magnetic probes and 8 saddle loops, where a value of $\Lambda = \beta_p + (l_i - 1)/2$ is obtained, where β_p is poloidal beta value and l_i is internal inductance of the plasma. The value of l_i is determined as follows; assuming that the stored energy in ohmic plasma is proportional to a line average electron density \bar{n}_e , Λ is plotted as a function of \bar{n}_e and the Λ value at the extrapolated straight line with $\bar{n}_e = 0$ is assumed $\beta_p = 0$.

3. EXPERIMENTAL RESULTS.

3.1 General feature of heating

Temporal evolution of the plasma parameters during 1.2 MW ICRF heating is shown in Fig. 1. The plasma current is 225 kA and $\kappa = 1.2$. The density increases from 3 to $5 \times 10^{19} \text{ m}^{-3}$ during the heating pulse due to intense gas puffing. The loop voltage decreases from 1.7 to 0.8 V. The central electron temperature measured by Thomson scattering increases from 0.8 keV just before the heating to 1.9 keV at peak value and then decreases gradually. The poloidal beta value, however, continues increasing during the heating pulse. Therefore, the decay of the electron temperature is considered to be the results of the rapid increase of electron density. The deuterium temperature measured by a mass separated charge exchange neutral analyser increases from 0.5 to 0.9 keV, the increment is much smaller compared to the increase of electron temperature. This results indicates that strong electron heating occurs as is expected from mode conversion theory[12].

A total stored energy increases almost linearly as rf input power increases as shown in Fig. 2. The plasma current is 390 ~ 400 kA and $\kappa = 1.4$. Up to 2.1 MW of heating power, the increase of the stored energy has not tendency to saturate. The joule input power at 2.1 MW heating is 360 kW. Therefore the additional heating power is about 6 times as large as joule input power. At the maximum heating power, the total stored energy is achieved to be 74 kJ and the average toroidal beta value $\langle \beta_T \rangle$ is 2.2 %, which is about 75 % of critical beta value $\beta_c (= 0.3 I_p (\text{kA}) / a(\text{cm}) B_T(t))$ [13].

3.2 Dependence on Density and Plasma Current

Fig. 3 shows the total stored energy as a function of electron density for cases of $I_p = 415$ kA(a) and $I_p = 320$ kA(b). Open circles and solid circles show the stored energy in ohmic and in about 1 MW rf heated plasma, respectively. The stored energy in the ohmic plasma is proportional to the electron density. This indicates that the energy confinement time in the ohmic plasma τ_E^{OH} follows Alcator type scaling [14], where τ_E^{OH} is proportional to the electron density.

The stored energy at additional heating phase increases linearly as the density increases. Those two straight lines are almost parallel, that is, the difference of the stored energy between the ohmic and the additional heated plasma W_{ad} is constant irrespective to the electron density in both $I_p = 415$ kA and $I_p = 320$ kA cases.

The increment of the stored energy W_{ad} by about 1 MW ICRF heating is plotted as a function of plasma current in Fig. 4. W_{ad} is almost constant for the plasma current. Thus, the increment of stored energy by the ICRF heating is independent of the plasma current and the electron density.

Assuming that the stored energy in the ohmic plasma W_{OH} is proportional to the density up to more higher density in the additional heating phase, W_{ad} is defined as a difference between the total stored energy W_T and W_{OH} as follows

$$W_{\text{ad}} = W_T - W_{\text{OH}}(\bar{n}_e) \quad (3)$$

W_{ad} is plotted as a function of the ICRF heating power in the case of Fig. 2 as shown in Fig. 5. The increment of stored energy by the ICRF heating W_{ad} increases in proportion to the rf heating power up to the maximum power 2.1 MW.

Experimental results shown in Figs. 3, 4 and 5 support the hypothesis which the ICRF heated plasma consist of two parts in view of energy confinement, those are, ohmic base plasma and the increment part by the additional heating.

3.3 Transient Characteristic of the Stored Energy

If the increment part by the additional heating behaves independently of the ohmic base plasma, a transient properties, that is, a characteristic time of the total stored energy decrease (or increase) should be different from the gross energy confinement time. In order to measure the energy decay time, NBI heating is superimposed to the steady state ICRF heated plasma. ICRF power is injected from 600 to 900 ms. The neutral beam with 0.8 MW is injected at 750 ms with 50 ms pulse width. After the neutral beam is terminated, the stored energy decays exponentially to a steady state ICRF heated value. Examples of temporal evolution of stored energy are shown in Fig. 6. Figure (a) shows a case of ICRF power $P_{\text{ICRF}} = 120$ kW, then gross energy confinement time $\tau_E^G = 46$ ms, (b) $P_{\text{ICRF}} = 570$ kW, $\tau_E^G = 28$ ms and (c) $P_{\text{ICRF}} = 1400$ kW, $\tau_E^G = 21$ ms. For all cases, the stored energy decays roughly exponentially with almost the same time.

A gross energy confinement time τ_E^G changes from 46 ms at ohmic heating to 21 ms at 1.45 MW ICRF heating as shown in Fig. 7. Open circles represent τ_E^G at ICRF heating phase and solid circles represent τ_E^G at ICRF plus 0.8 MW NBI heating phase. The gross energy confinement time decreases almost inverse proportional to square root of total input power as indicated solid lines in the figure. This power dependence is almost the same as the results obtained other tokamaks. The absolute value is about 10 % less than the Kaye-Goldston scaling[6], but the power dependence is almost fit to the scaling.

On the other hand, the decay time of stored energy is almost constant as shown in Fig. 8. These values are spread from 13 ms to 16 ms with no systematic dependence on ICRF power. This experiment directly proves that the characteristic time of the total stored energy decrease does not coincides with the gross energy confinement time and proves from the other side that the ICRF heated plasma consist of two parts, in view of energy confinement time.

The stored energy in the ohmic plasma is shown in Fig. 9. W_{OH} is proportional to the plasma density but the increase saturates at the density larger than $3.5 \times 10^{19} \text{ m}^{-3}$. Using this density dependence of W_{OH} ,

the increment of stored energy by the ICRF heating W_{ad} is plotted in Fig. 10. Open circles represent W_{ad} at ICRF heating only at just before and sufficiently after the NBI pulse. Solid circles represent W_{ad} at ICRF plus 0.8 MW NBI heating. W_{ad} at ICRF heating is proportional to the ICRF input power with the inclination 13 kJ/MW which is almost the same in the case of $I_p = 400$ kA shown in Fig. 5.

W_{ad} at ICRF plus 0.8 MW NBI heating is about 11 kJ larger than that at ICRF heating only and this value is correspond to that at 0.8 MW ICRF heating. This results indicates that these two heating method are completely additive and that, at least of this case, heating efficiencies of ICRF and NBI are the same.

3.4 Confinement Model and Point Model Simulation.

We can construct the following confinement model of the ICRF heated plasma from experimental data shown in III-2 and III-3.

The additionally heated plasma consists of two parts. The one is ohmic base plasma and the other is the increment part by the ICRF heating as shown in Fig. 11. These two plasmas are almost independent on the point of view of transport property.

Stored energy of the ohmic base plasma is proportional to the density and a function of plasma current (almost proportional to plasma current), and perhaps, a function of minor and major radius. Stored energy of the increment part by the ICRF heating is proportional to the additional heating power, and is independent of the plasma current and the density. An interaction between these two plasmas may occurs through a decrease of joule input power, resulting from increase of electron temperature by the ICRF heating. The decrement of the joule input power may be supplied from the additional heating power.

Assuming this hypothesis, a power balance equation can be written by the following;

$$W_T = W_{OH} + W_{ad} \quad (4)$$

$$\frac{dW_{ad}}{dt} = P_{ad} - \Delta V_L I_p - \frac{W_{ad}}{\tau_{ad}} \quad (5)$$

$$\tau_{ad} = W_{ad} / (P_{ad} - \Delta V_L I_p) \Big|_{\text{steady state}} = \Delta W_T / \Delta P_{\text{Tot}} \Big|_{\bar{n}_e} = \text{const.}$$

where P_{ad} is additional heating power and $\Delta V_L I_P$ is the decrement of joule input power by the additional heating.

W_{OH} is understood as a capacity of stored energy in the ohmic base plasma, and is proportional to the electron density but the increase saturates when the density exceeds an critical density \bar{n}_c . The critical density increases as the plasma current increases, but the functional dependence on the plasma current is not clear yet. In the present analysis, W_{OH} is determined by a simple extrapolation to the higher density from the value obtained in the ohmic plasma without additional heating.

τ_{ad} is the energy confinement time of the additionally heated part of the plasma and is response time of the stored energy increase or decrease when the additional heating power changes. Equations (4) and (5) teach us that in sufficiently high power heating experiment such as $W_{OH} \ll W_{ad}$, the gross energy confinement time should be agree with τ_{ad} . Therefore, it is important to establish the scaling of τ_{ad} for a extrapolation to large and high power heating experiment. Up to now, it was shown that τ_{ad} is independent of plasma current, electron density and additional heating power, given by,

$$\tau_{ad} \propto I_P^0 \bar{n}_e^0 \cdot P_{ad}^0$$

Fig. 12 shows W_{ad} as a function of $(P_{ICH} - \Delta V_L I_P)$. The inclination gives energy confinement time of W_{ad} . The value is 15 ms, and is roughly coincides with the decay time of the stored energy shown in Fig. 8.

Using power balance equations (4) and (5), and putting $\tau_{ad} = 15$ ms, time evolution of the total stored energy is simulated as shown in Fig. 13, where Fig. (a) shows ICRF and NBI heating phase and Fig. (b) ICRF heating only. The thick line in W_T is experimental value and the thin line is the simulated one. The broken line represents W_{OH} . The experimental values and the simulated values are well agree in increasing and decreasing phase by ICRF and NBI heating and also in steady state phase. This result indicates that the confinement model is applicable to the NBI heated plasma.

3.5 Improved Confinement Case

Sometimes, abrupt increase of radiation loss is observed as shown in Fig. 14. Preceding the burst of the radiation loss (P_R), antenna loading resistance (R_p) abruptly increase, which is a indication of electron density increase around antennae. After this phenomena quiets down, the radiation

loss and one turn voltage (V_L) decrease gradually, and the total stored energy (W_T) increases. This phenomena occurs with intense gas puffing and with high power heating typically larger than 1 MW, but does not always occurs in such conditions.

In this case, the peak value of the total stored energy is larger than the value expected by the two plasma model. Figure 15 shows W_{ad} as a function of P_{ICH} before the radiation burst (o), and after the radiation burst the peak values of the stored energy is plotted by solid circles. Open circles indicates that W_{ad} is almost the same value as Fig. 5 and 10, but those solid circles are larger than the standard value by about 10 kJ.

We cannot conclude that either W_{OH} or W_{ad} contributes the increase of total stored energy. There is a possibility that large increase of radiation loss changes current profile slightly, and the change of the current profile changes a standard value of W_{ad} or W_{OH} .

4. DISCUSSIONS AND SUMMARY

4.1 Cause of Confinement Deterioration

Experimental results shown in this paper indicates that the ICRF heated plasma can be considered to consist of two parts, those are, ohmic base plasma and the increment part by the ICRF heating. A characteristic response time of the stored energy when the additional heating power changes does not agree with gross energy confinement time but with the energy confinement time of the incremental energy. A concept that the transport of the plasma is deteriorated gradually as the heating power or the plasma pressure is denied. The cause of the deterioration is that the energy confinement time of the additionally heated part of the plasma is small compared to that of ohmic base plasma.

We cannot draw the physical picture how the increment part by the additional heating behaves independently of the ohmic base plasma. This phenomena may be understood as one side view of the "profile consistency", where there is an almost same question how the plasma changes its transport properties so as to maintain the optimum current density in the ohmic plasma. In order to answer these questions and to improve the confinement during additional heating, it is important to control the current profile by some other method of ohmic heating. The improvement of confinement shown in III-5 may be considered as a preliminary indication

loss and one turn voltage (V_L) decrease gradually, and the total stored energy (W_T) increases. This phenomena occurs with intense gas puffing and with high power heating typically larger than 1 MW, but does not always occurs in such conditions.

In this case, the peak value of the total stored energy is larger than the value expected by the two plasma model. Figure 15 shows W_{ad} as a function of P_{ICH} before the radiation burst (o), and after the radiation burst the peak values of the stored energy is plotted by solid circles. Open circles indicates that W_{ad} is almost the same value as Fig. 5 and 10, but those solid circles are larger than the standard value by about 10 kJ.

We cannot conclude that either W_{OH} or W_{ad} contributes the increase of total stored energy. There is a possibility that large increase of radiation loss changes current profile slightly, and the change of the current profile changes a standard value of W_{ad} or W_{OH} .

4. DISCUSSIONS AND SUMMARY

4.1 Cause of Confinement Deterioration

Experimental results shown in this paper indicates that the ICRF heated plasma can be considered to consist of two parts, those are, ohmic base plasma and the increment part by the ICRF heating. A characteristic response time of the stored energy when the additional heating power changes does not agree with gross energy confinement time but with the energy confinement time of the incremental energy. A concept that the transport of the plasma is deteriorated gradually as the heating power or the plasma pressure is denied. The cause of the deterioration is that the energy confinement time of the additionally heated part of the plasma is small compared to that of ohmic base plasma.

We cannot draw the physical picture how the increment part by the additional heating behaves independently of the ohmic base plasma. This phenomena may be understood as one side view of the "profile consistency", where there is an almost same question how the plasma changes its transport properties so as to maintain the optimum current density in the ohmic plasma. In order to answer these questions and to improve the confinement during additional heating, it is important to control the current profile by some other method of ohmic heating. The improvement of confinement shown in III-5 may be considered as a preliminary indication

that a little change of the current profile improving the confinement properties.

4.2 Effect of Plasma Current

The incremental confinement time τ_{ad} is independent of the plasma current as shown in the present experiment. But the total stored energy (or the gross energy confinement time) improves as the plasma current, because W_{OH} increases as increasing the plasma current. Even in the case of sufficiently large additional heating power compared to joule input power, a contribution of W_{OH} in the total stored energy is still large. For example, in the case of Fig. 2 at 2.1 MW heating, $P_{ICH}/P_{OH} = 6$, on the other hand $W_{ad}/W_{OH} = 0.7$. This results shown that the large value of P_{ad}/P_{OH} ratio is not a indication that the plasma is free from the joule heating.

PLT ICRF heating experiment shows strong improvement by the plasma current. In that case, minority heating regime is used. In order to expect a good heating results, a confinement of high energy minority ions by the high plasma current is necessary. Therefore, effective absorbed power increases as the plasma current increases.

4.3 Validity of two plasma model

Experimental results shown in this paper are mainly obtained in a electron heating regime of ICRF heating, but the present two plasma model may be applicable to the NBI heated plasma as shown in 3.3 and 3.5, and also applicable to the other tokamaks. JET ICRF heating experiment shows that energy decay time of 250 ms is coincides with a steady state confinement time of the additional heating power deduced from $\Delta W_T/\Delta P_{Tot}$ [4].

4.4 Summary

If the present confinement model is valid for all tokamak and for all additional heating method, previous scaling studies to predict the gross energy confinement time has the significance in only interpolation of plasma parameters, and for the extrapolation to large and high power heating experiment, it is necessary to establish the scaling of τ_{ad} . It was shown that the confinement time of additional heating power is independent of plasma current, electron density and additional heating power, that is,

$$\tau_{ad} \propto I_P^0 n_e^0 P_{ad}^0$$

Acknowledgement

The authors are grateful to the members of the JFT-2M operation group for their excellent operation and helpful supports. Stimulating discussions with Drs. K. Itoh (Heliotron Group PPI, Kyoto Univ.), S. I. Itoh (Inst. for Fusion Theory, Hiroshima Univ.) and T. Takizuka are gratefully acknowledged. We also sincerely thanks to Drs. A. Funahashi, M. Tanaka and Y. Tanaka for their continuous encouragement.

References

1. M. Mori, et al., Plasma Phys. and Contr. Nucl. Fusion Res. (IAEA, Vienna, 1985) Vol. 1, 445.
2. J. Hosea, et al., Proc. 12th Euro. Conf. on Contr. Fusion and Plasma Phys. (Budapest, Sept. 1985) 120.
3. K. Steinmetz, et al., *ibid.*
M. Keilhacker, et al., *ibid.*, Invited Paper "Confinement in ASDEX with Neutral Beam and RF Heating."
4. J. Jaquinot, et al., *ibid.*, Invited Paper "ICRF Studies on JET".
5. A.M. Messiaen, et al., *ibid.*, Invited Paper.
6. S.M. Kaye and R.J. Goldston, Nucl. Fusion 25 (1985) 65.
7. R.J. Goldston, Plasma Phys. and Contr. Fusion 26 (1984) 87.
8. B. Coppi, Comments Plasma Phys. and Contr. Fusion, 5 (1980) 201.
9. E. Speth, et al., Proc. 12th Euro. Conf. on Contr. Fusion and Plasma Phys. (Budapest, Sept. 1985) 284.
10. H. Tamai, et al., "Impurity Suppression during the ICRF Heating in the JFT-2M Tokamak" to be published in Nucl. Fusion.
11. D.W. Swain and G.H. Neilson, Nucl. Fusion, 22 (1982) 1015.
12. A. Fukuyama, et al., Nucl. Fusion 23 (1983) 1005.
13. F. Troyon et al., Plasma Phys. and Contr. Fusion, 26 (1984) 209.
14. D.L. Jassby, et al., Nucl. Fusion, 16 (1976) 1045.

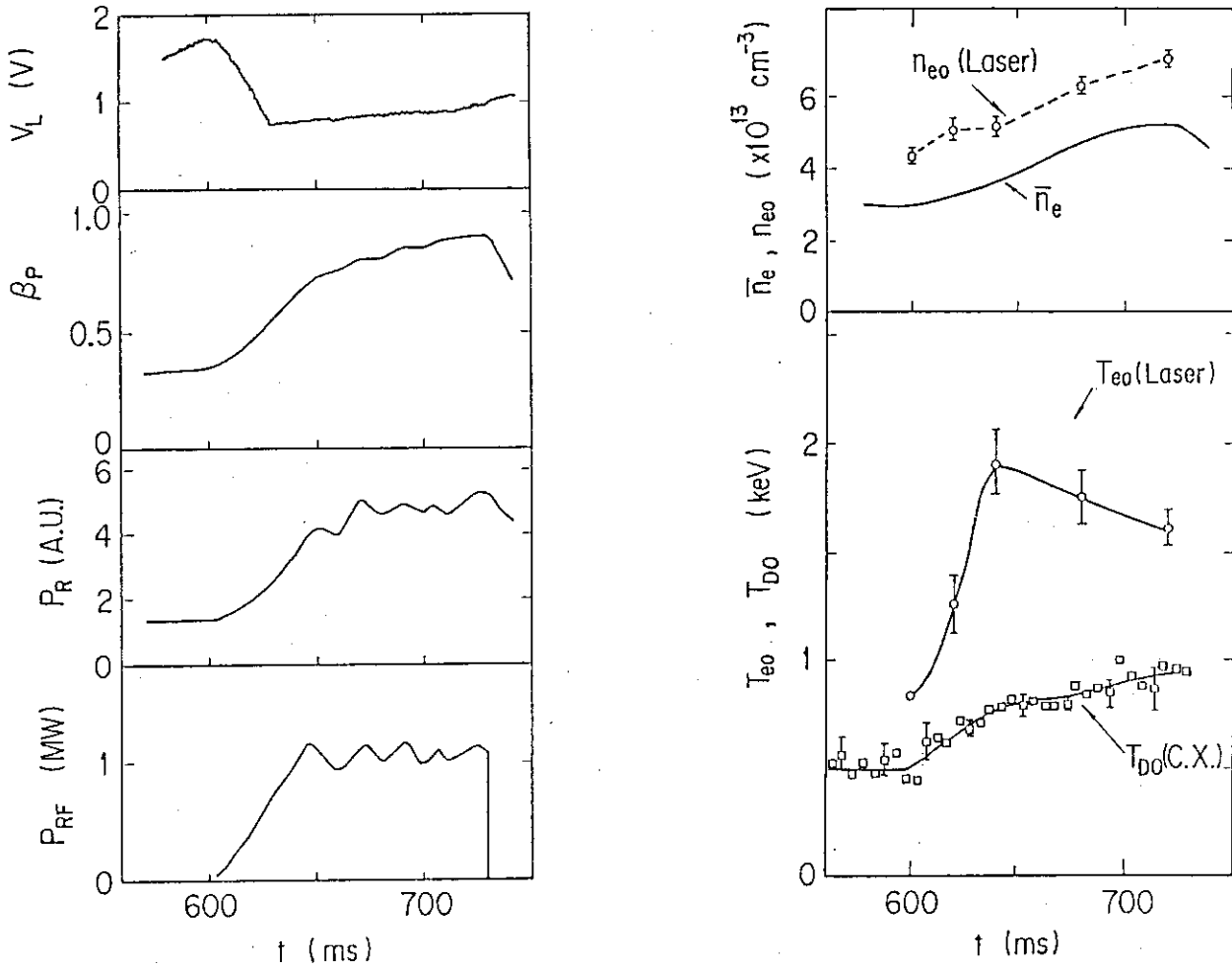


Fig. 1 Temporal evolution of plasma parameters during 1.2 MW ICRF heating. Plasma current $I_p = 225$ kA and $\kappa = 1.2$.

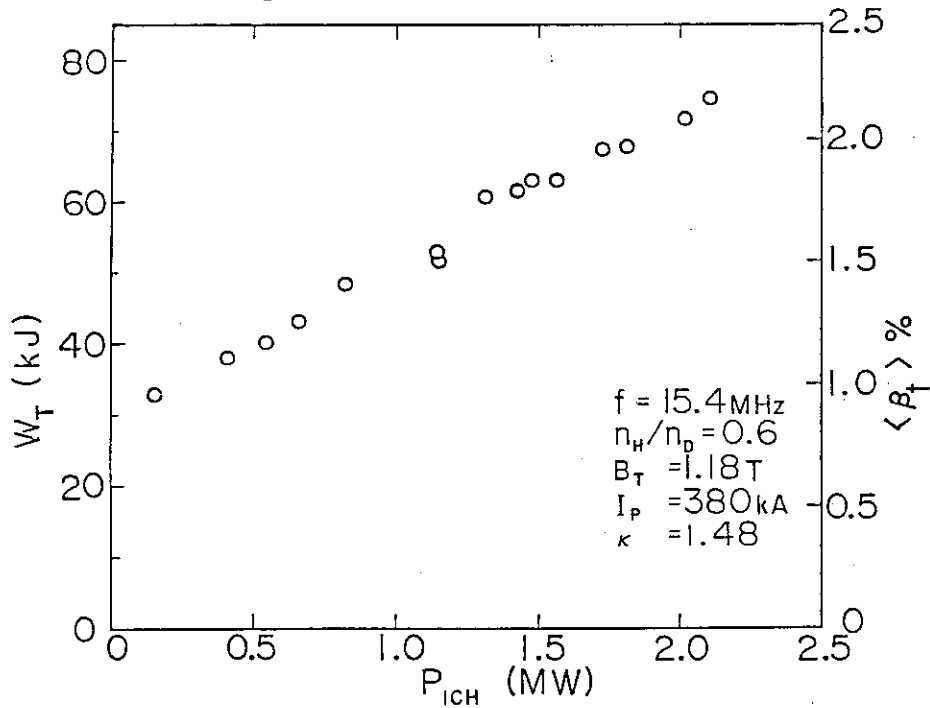


Fig. 2 Total stored energy as a function of ICRF heating power. Line average density increases from $4 \times 10^{19} \text{ m}^{-3}$ in low power to $7 \times 10^{19} \text{ m}^{-3}$ in 2 MW heating.

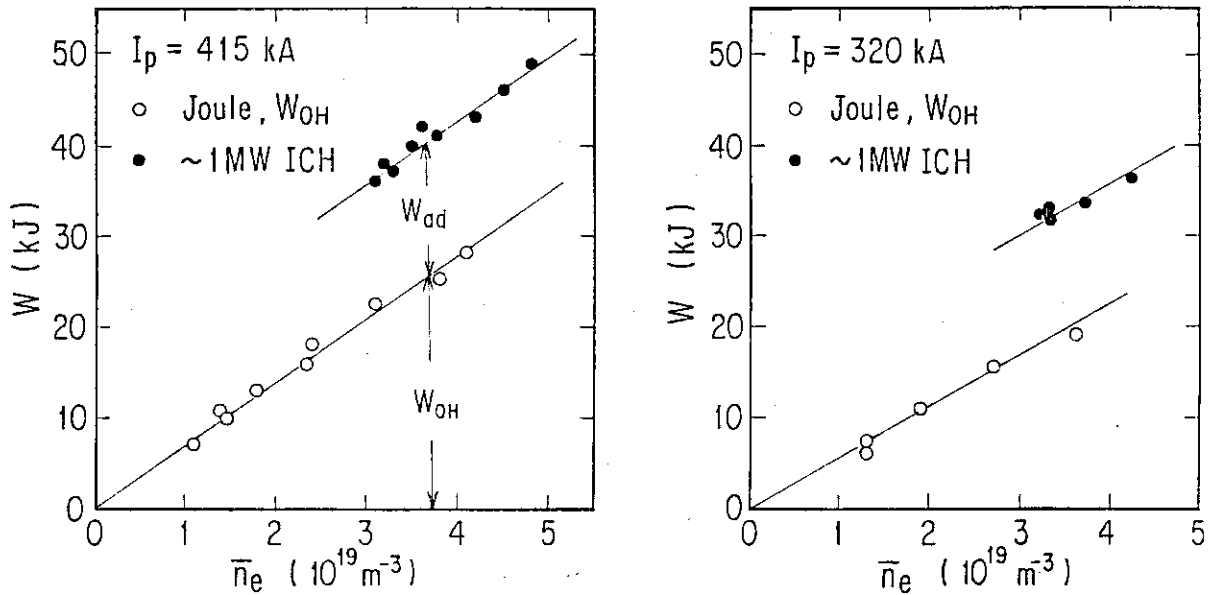


Fig. 3 Total stored energy as a function line average density \bar{n}_e , during ohmic (\circ) and about 1 MW ICRF (\bullet) heating. The increment of stored energy W_{ad} is constant to the plasma density.

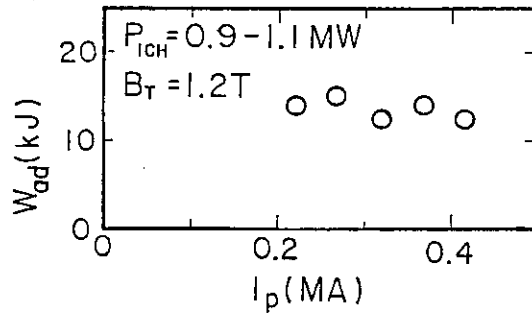


Fig. 4 Increment of stored energy W_{ad} by about 1 MW ICRF heating is plotted as a function of plasma current I_p . W_{ad} is roughly constant to the plasma current.

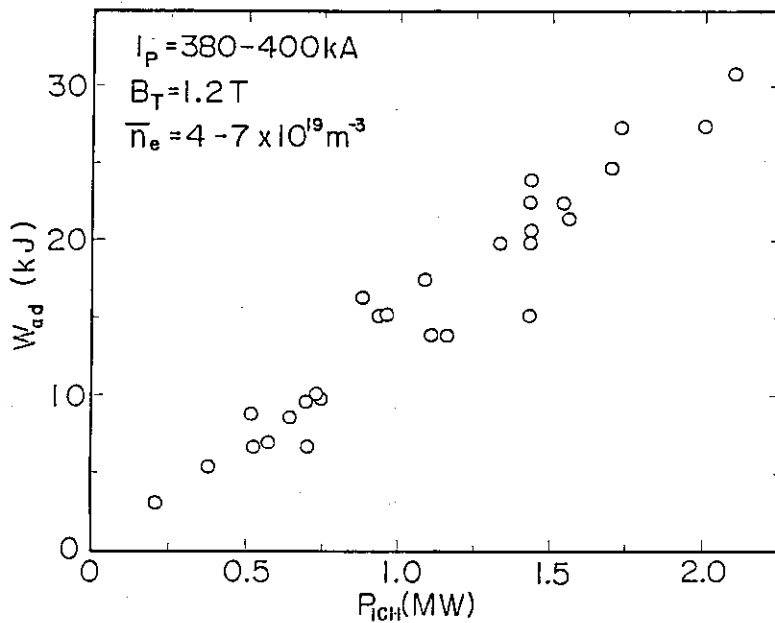


Fig. 5 W_{ad} is plotted as a function of ICRF heating power in the case of Fig. 2, where W_{ad} is defined by $W_{ad} = W_T - W_{OH}(\bar{n}_e)$. $W_{OH}(\bar{n}_e)$ is extrapolated value from joule heating phase.

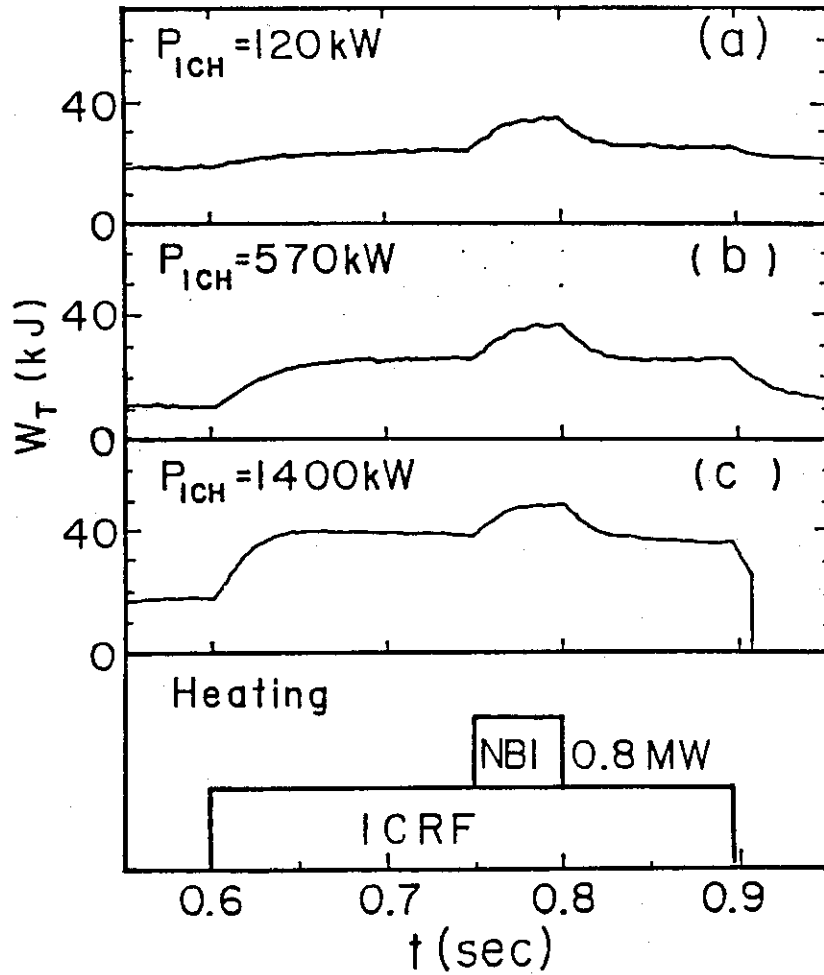


Fig. 6 Temporal evolution of total stored energy, when NBI heating is superimposed to the steady state ICRF heated plasma. Fig. (a) shows a case of ICRF power $P_{\text{ICH}} = 120$ kW, then gross energy confinement time $\tau_{\text{E}}^{\text{G}} = 46$ ms, (b) $P_{\text{ICH}} = 570$ kW, $\tau_{\text{E}}^{\text{G}} = 28$ ms and (c) $P_{\text{ICH}} = 1400$ kW, $\tau_{\text{E}}^{\text{G}} = 21$ ms. For all cases, the stored energy decays roughly exponentially with almost the same time.

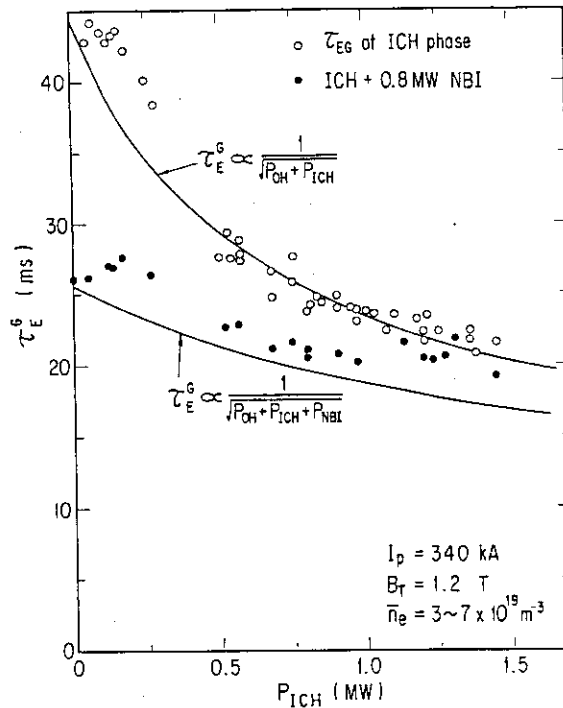


Fig. 7 Gross energy confinement time τ_E^G as a function of ICRF heating power. Open circles represent τ_E^G at ICRF heating phase and solid circles at ICRF plus 0.8 MW NBI heating. τ_E^G decreases almost inverse proportional to square root of total input power as indicated solid lines in the figure.

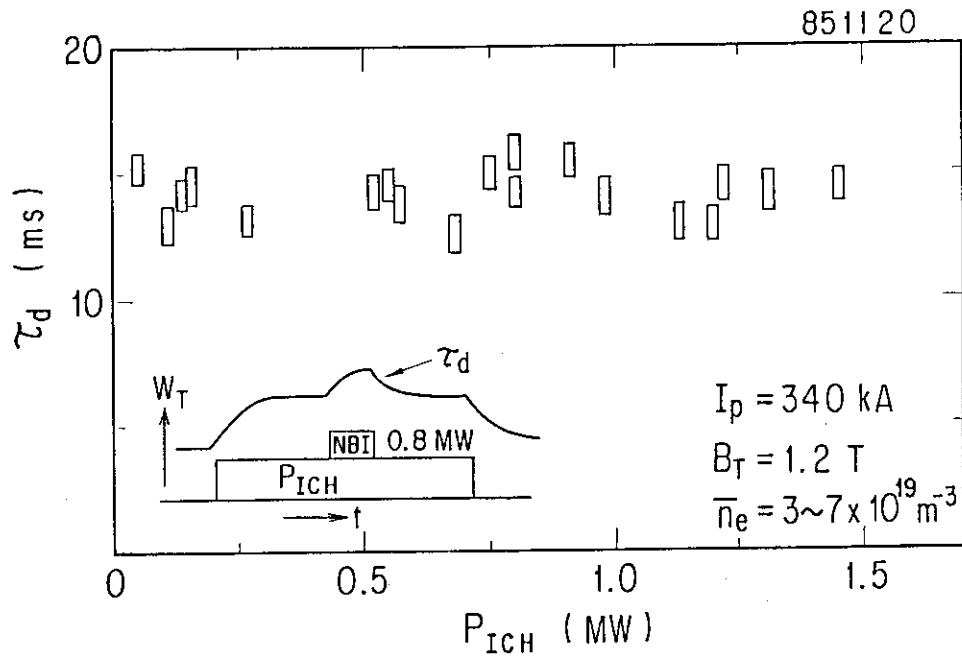


Fig. 8 Decay time of stored energy τ_d when NBI is terminated, as a function of ICRF heating power. τ_d is almost constant irrespective to τ_E^G which changes from 46 ms to 21 ms.

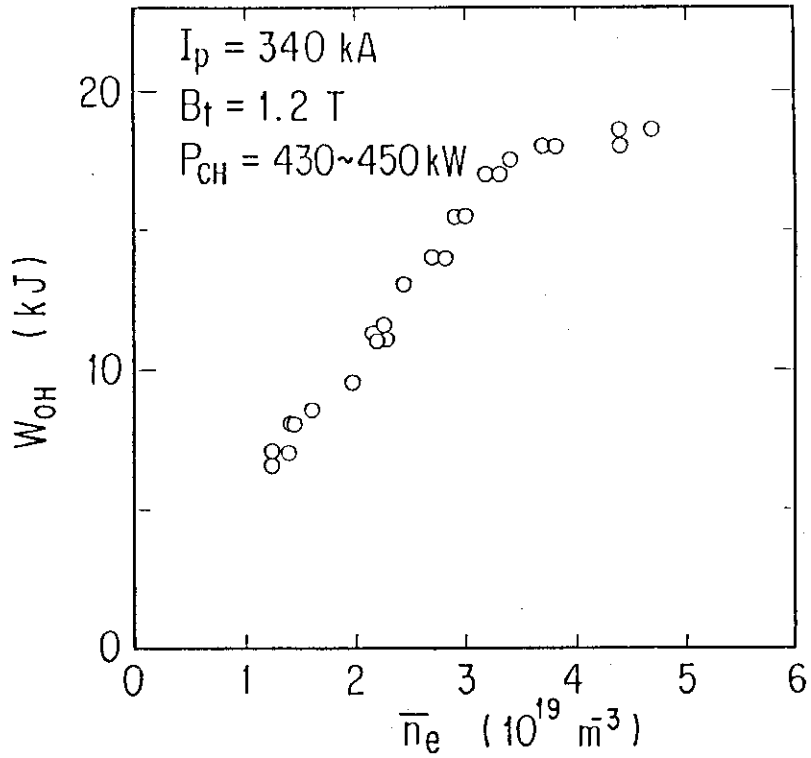


Fig. 9 Stored energy in the ohmic plasma as a function of \bar{n}_e , in the case of Fig. 6 and 7.

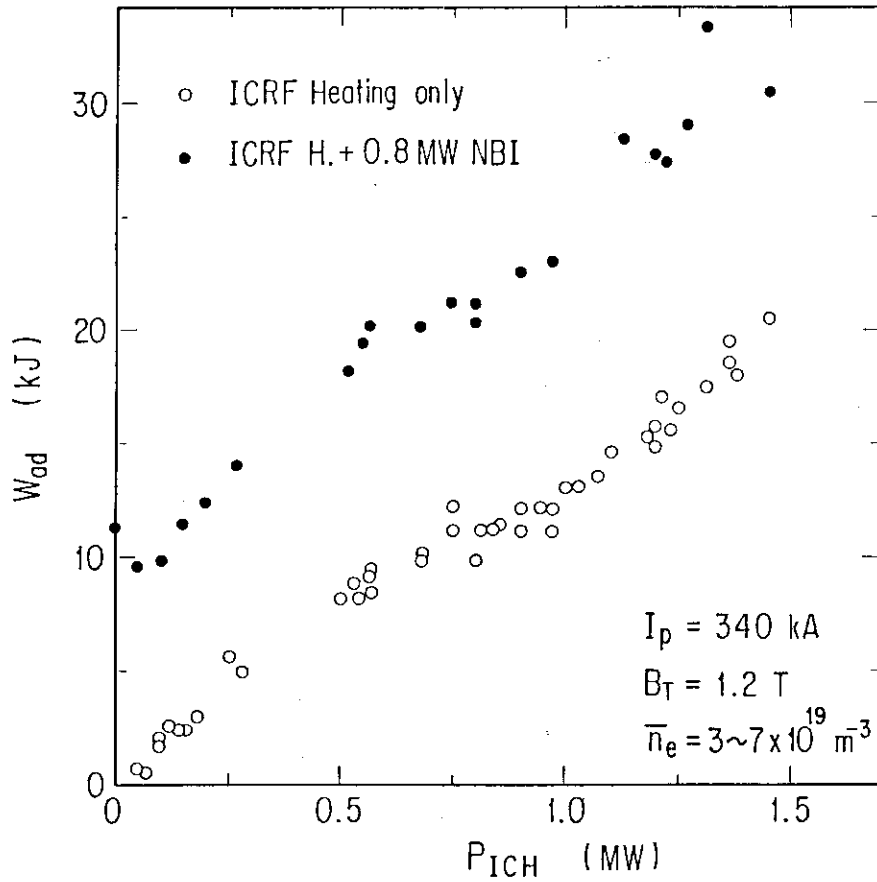


Fig. 10 W_{ad} as a function of ICRF heating power using density dependence of W_{OH} shown in Fig. 9. W_{ad} at ICRF plus 0.8 MW NBI heating is also plotted by solid circles.

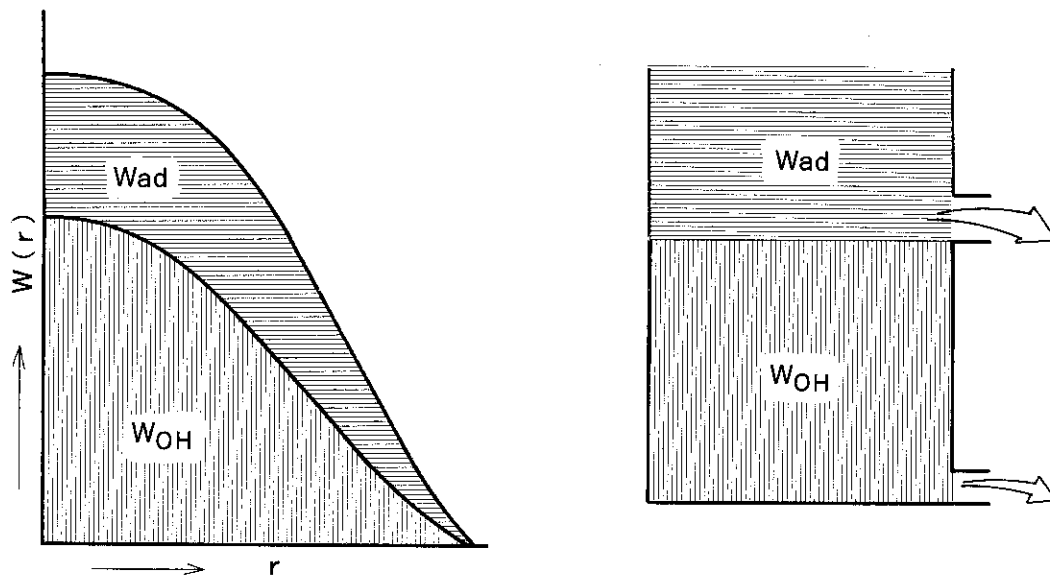


Fig. 11 Conceptual confinement model. The additional heated plasma consists of two parts, those are, ohmic base plasma and increment part by the additional heating. These two plasmas are almost independent on the point of view of transport properties.

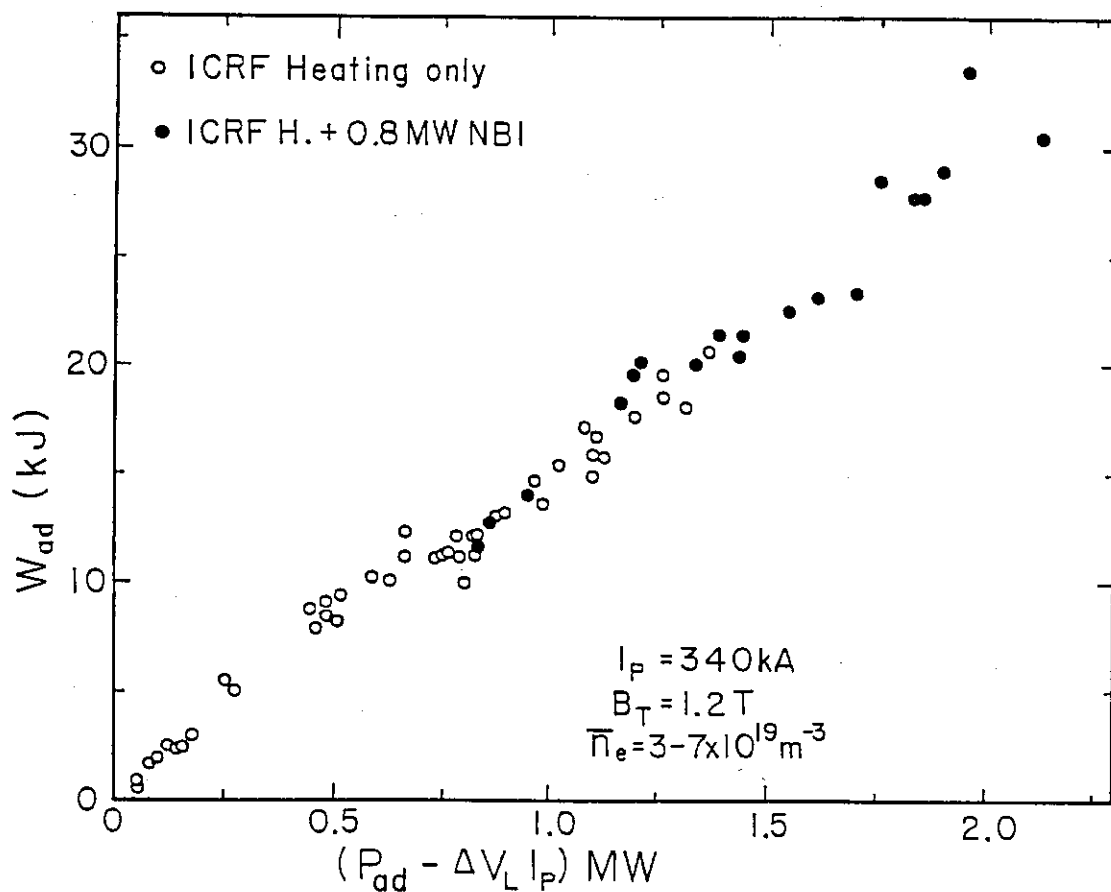


Fig. 12 W_{ad} as a function of $(P_{ad} - \Delta V_L I_P)$. The slope gives $\tau_{ad} = 15 \text{ ms}$.

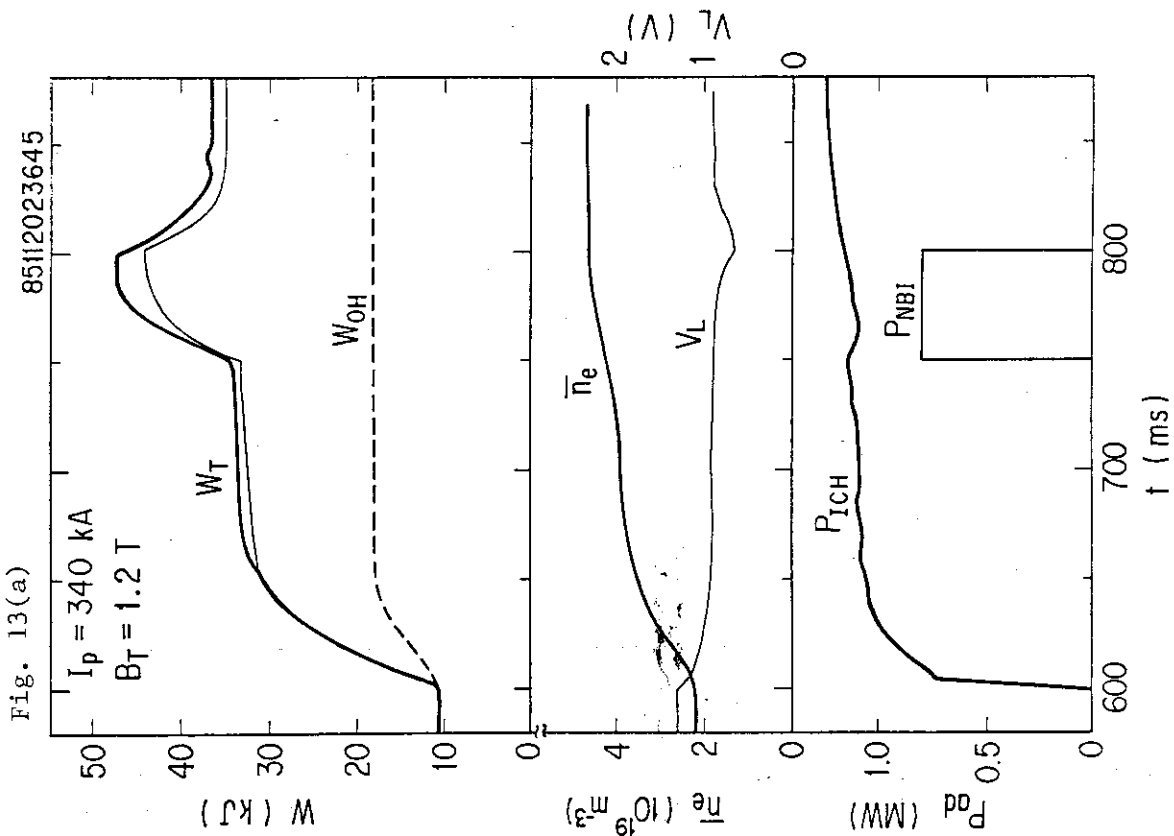
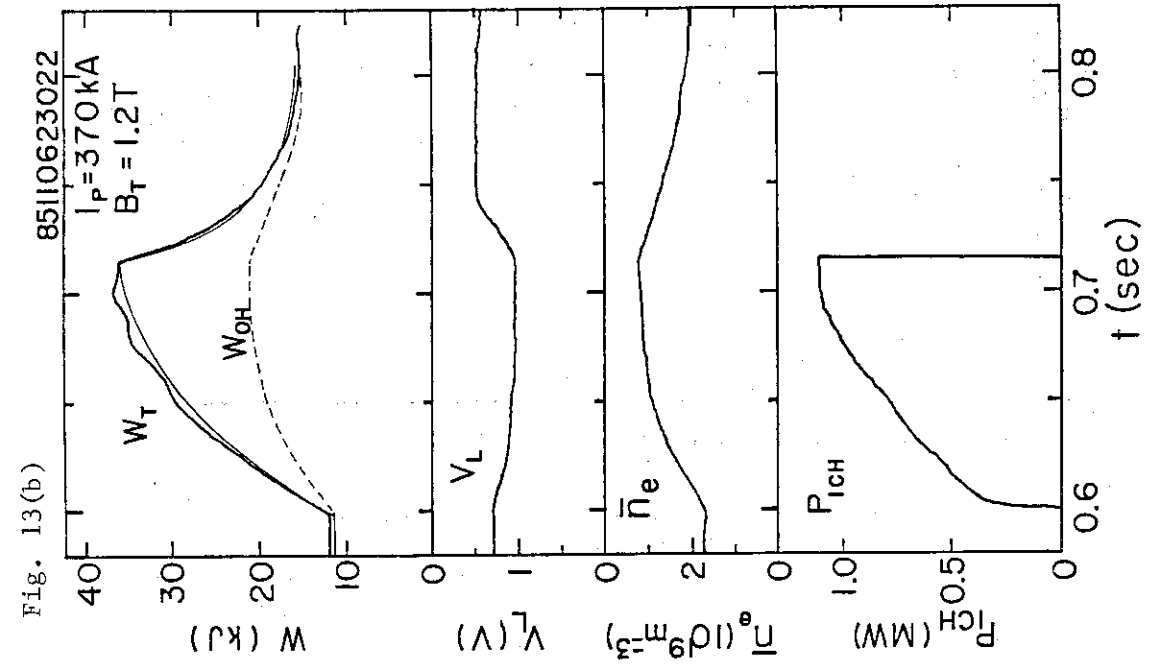


Fig. 13 Temporal evolution of stored energy W_T (thick line) is compared with a simulated value (thin line) using Eq. (4) and (5).

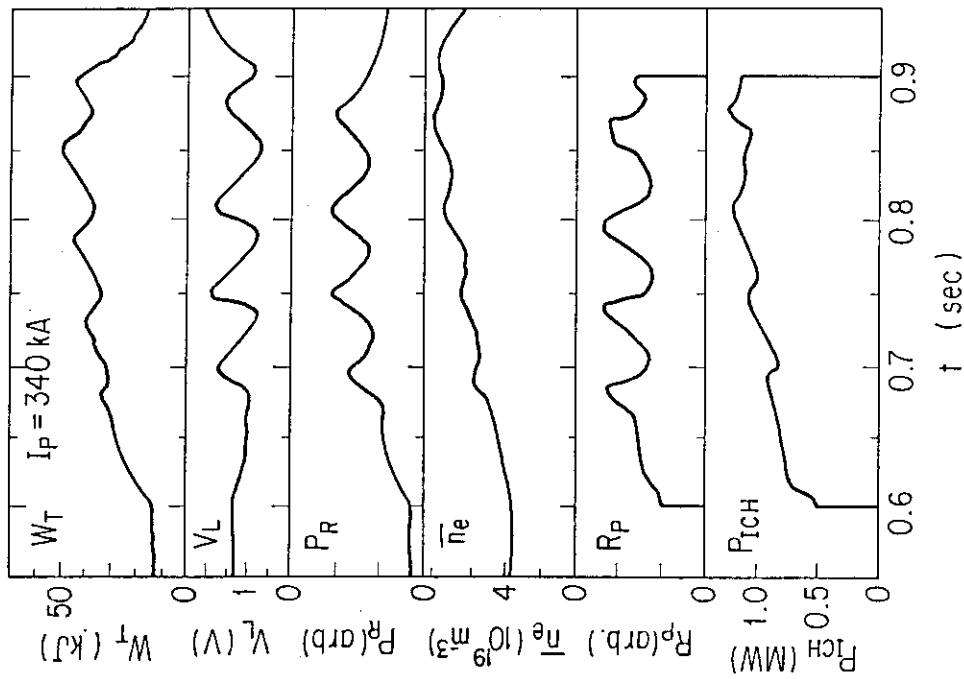


Fig. 14 Temporal evolution of plasma parameters in the case of abrupt increase of radiation loss.

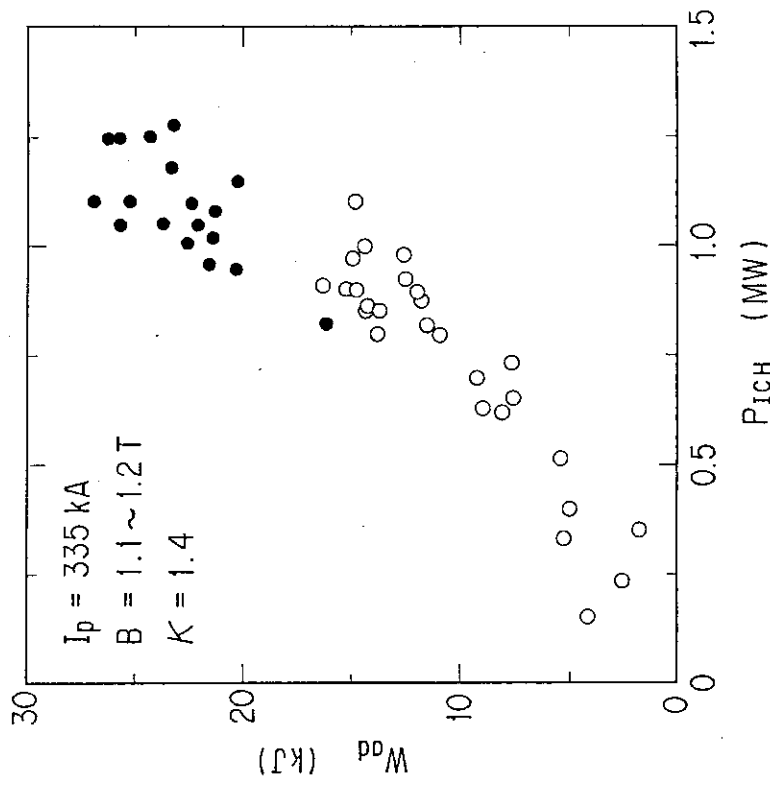


Fig. 15 W_{ad} vs. P_{ICH} , at before the radiation burst occurs (\circ) and after the burst, peak value of the stored energy (\bullet).